ISSN: 2634-9221
European Journal of Applied Sciences; Vol. 14 No. 03 (2026) (261-278)
https://doi.org/10.14738/aivp.1403.1266

Climatic Teleconnections and Fire Hotspot Seasonality in Bolivia (2000–2025): Association with Niño 3.4, PDO, and SAM Indices

Guillermina Miranda Torrez, M.Sc., Ing.

1. Institute of Ecology – Universidad Mayor de San Andrés (UMSA), Bolivia

Abstract: The occurrence of fire hotspots in Bolivia results from a complex interaction between regional climatic seasonality and large-scale ocean–atmosphere variability. The objective of this study was to analyze the relationship between global climate indices and the monthly dynamics of fire hotspots across four Bolivian biomes during the period 2000–2025. This was achieved through time-series analysis, the calculation of the Seasonal Variation Index (SVI), and the evaluation of monthly variability in local meteorological variables. A quantitative, observational, longitudinal, and retrospective approach was adopted, based on monthly series of fire hotspots, maximum temperature, minimum relative humidity, and maximum wind speed from the meteorological stations of El Alto, Cochabamba, Viru Viru, and San José de Chiquitos. Temporal characterization included descriptive statistics, Sen's slope estimator, autocorrelation functions, and the Ljung–Box test, while intra-annual seasonality was examined using the SVI. Furthermore, associations between the Niño 3.4 index, the Pacific Decadal Oscillation (PDO), and the Southern Annular Mode (SAM) with local meteorological variables were estimated using Pearson correlations with lags ranging from 0 to 5 months. The results revealed a non-random temporal structure dominated by a persistent annual periodicity and, in several cases, a secondary biennial signal. The SVI indicated that fire hotspot activity was seasonally concentrated between August and October, with a principal peak in September, coinciding with positive anomalies in maximum temperature and negative anomalies in minimum relative humidity. In the association analysis, the Niño 3.4 index exhibited the strongest positive correlations with maximum temperature, particularly in Cochabamba, whereas the SAM displayed the clearest inverse signal with minimum relative humidity in El Alto. The PDO showed weaker and more heterogeneous associations. It is concluded that the monthly dynamics of fire hotspots in Bolivia are strongly structured by climatic seasonality, and that local meteorological variability exhibits differential associations with global climate forcings. This provides an analytical foundation useful for seasonal monitoring and wildfire risk management.

Keywords: Fire hotspots, climatic teleconnections, seasonality, time series, Seasonal Variation Index (SVI).

INTRODUCTION

The intensification, greater seasonal persistence, and spatial expansion of vegetation fires constitute one of the most notable features of the contemporary context of climate change. Their occurrence does not result from a single factor but rather from the nonlinear interaction among large-scale atmospheric forcings, local meteorological conditions, fuel moisture status, and ignition sources. From the perspective of fire climatology, risk increases when elevated temperatures, low atmospheric humidity, antecedent hydric deficit, and strong winds converge, as this combination accelerates the desiccation of fine

fuels, enhances their flammability, and favors fire spread. In this regard, recent reports have documented an increase in warm and dry extremes and particularly severe fire seasons at the global scale, including South America, consolidating fire activity as an ecological, atmospheric, territorial, and socio-economic problem (Arguez et al., 2025).

The state of the art indicates that fire regimes depend not only on local controls but also on climatic teleconnections that modulate temperature, regional circulation, and moisture availability, thereby influencing the seasonality of fire-conducive conditions. Cardil et al. (2023) demonstrated that such teleconnections explain a significant proportion of the global burned area, although responses vary across continents and biomes. Among the principal forcings are the El Niño–Southern Oscillation (ENSO), a robust interannual modulator; the Southern Annular Mode (SAM), the dominant mode of extratropical variability in the Southern Hemisphere, linked to changes in the intensity and latitudinal position of the westerlies; and the Pacific Decadal Oscillation (PDO), which introduces low-frequency modulation into the Pacific ocean–atmosphere system. In South America, research has advanced mainly through satellite products, burned area assessments, and hotspot detections, emphasizing the relationship between drought, thermal anomalies, and fire activity (Cardil et al., 2023).

In Bolivia, available evidence has described in greater detail the severity of recent fire seasons in the Amazon and Chiquitanía, as well as the combined influence of meteorological drought, land-use change, and forest fragmentation. Maillard et al. (2020) demonstrated, for Santa Cruz, that the spatial distribution of fires is closely associated with forest fragmentation and drought conditions, while Singh et al. (2022) identified spatial and temporal patterns of fire activity in the Bolivian Amazon and highlighted the scarcity of systematic studies for the country. Nevertheless, this evidence remains predominantly ecoregional, episodic, or focused on severe fire seasons.

The principal knowledge gap lies in the absence of a comparative, multi-biome characterization that integrates, within a single temporal scale, the monthly seasonality of fire hotspots with physically relevant local meteorological variables—maximum temperature, minimum relative humidity, and maximum wind speed—and with large-scale climate indices. This limitation is methodologically significant, as the analysis of associations in monthly series requires controlling for serial dependence and autocorrelation to avoid spurious inferences or overestimation of statistical significance.

In response, the present study proposes a multi-biome approach encompassing the Altiplano, Valleys, Chiquitanía, and Chaco to comparatively evaluate the large-scale climatic signal on the monthly dynamics of fire hotspots in Bolivia during 2000–2025. The physical basis rests on the fact that atmospheric warming increases the air's capacity to retain water vapor, thereby intensifying moisture deficits and promoting fuel desiccation; additionally, higher wind speeds enhance the potential for fire spread. Accordingly, the objective is to analyze the relationship between the Niño 3.4, PDO, and SAM indices and the monthly dynamics of fire hotspots through time-series analysis and the Seasonal Variation Index (SVI). It is hypothesized that the large-scale signal is not expressed homogeneously across Bolivia but rather through differentiated patterns of seasonal susceptibility according to biome and local meteorological context.

METHODOLOGY

Research Design and Approach

The study was structured under a quantitative framework, employing a non-experimental, observational, longitudinal, and retrospective design. This approach is appropriate for the analysis of hydroclimatic and atmospheric time series without manipulation of variables. The unit of analysis was the calendar month, and the observation period extended from January 2000 to December 2025, yielding 312 monthly observations per variable. The scope was descriptive–analytical, aimed both at characterizing the temporal structure of the series—trend, seasonality, periodicity, and serial dependence—and at examining their association with large-scale climatic forcings. Consequently, the analysis did not seek to establish causality but rather to identify patterns of covariation and temporal organization in accordance with classical procedures of statistical climatology and time-series analysis.

Study Area, Population, and Sample

The study area comprised the Plurinational State of Bolivia, considering four contrasting bioclimatic domains: Altiplano, Valleys, Chiquitanía, and Chaco, represented spatially in Figure 1. For each domain, a reference meteorological station was selected: El Alto, Cochabamba, Viru Viru, and San José de Chiquitos. Their comparative characteristics are summarized in Table 1. Selection was not based on probabilistic sampling but rather on technical representativeness, supported by the continuity of records, monthly homogeneity of information, completeness of the series, and institutional reliability of observations. This procedure enabled the construction of a comparative basis across physiographic and climatic regions, ensuring temporal and spatial consistency for multi-biome analysis.

Table 1: Geographic Attributes and Reference Climatological Parameters by Station

Station	Altitude (m a.s.l.)	Latitude (S)	Longitude (W)	Annual Temperature	Annual Precipitation	Biome
El Alto	4,135	16.5103	68.1986	7–9 °C	500–1600 mm	Altiplano
Cochabamba	2,564	17.4141	66.1827	12–16 °C	500–700 mm	Valleys
Viru Viru	378	17.6480	63.1370	21–28 °C	600–2300 mm	Chiquitanía
San José de Chiquitos	284	17.8322	60.7442	25–26 °C	400–900 mm	Chaco

Note: Adapted from Ibisch and Mérida (2003).

Variables Analyzed

Four primary variables were examined on a ratio scale. Monthly maximum temperature (Tmax) was expressed in degrees Celsius (°C), monthly minimum relative humidity (HRmin) in percentage (%), and monthly maximum wind speed (Vmax) in kilometers per hour (km/h). In addition, the variable fire hotspots was incorporated, defined as the monthly number of satellite detections of thermal anomalies recorded for Bolivia.

As large-scale climatic forcing variables, three indices widely employed in teleconnection studies were integrated: Niño 3.4, the Pacific Decadal Oscillation (PDO), and the Southern Annular Mode (SAM).

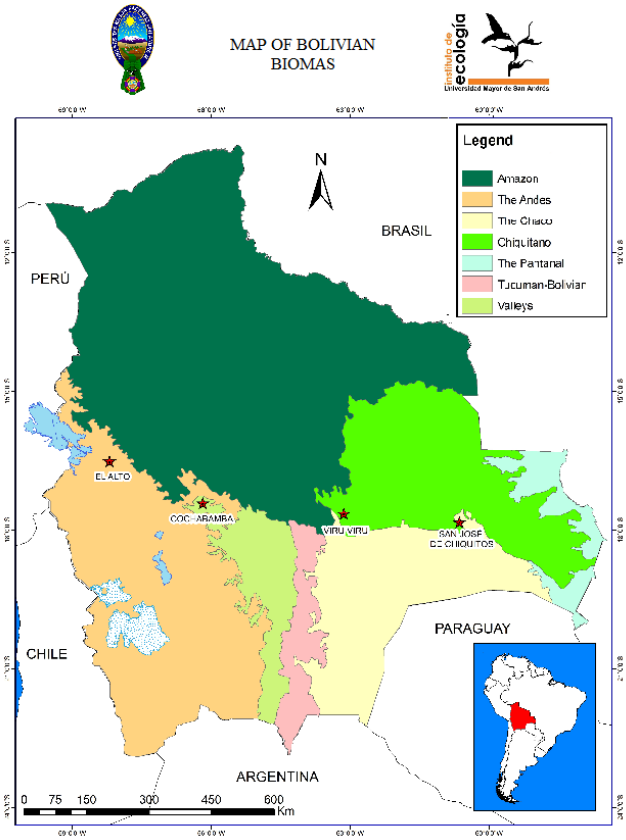

Data Sources and Information Collection

Information was obtained through documentary compilation from official secondary sources of recognized technical reliability. Local meteorological data were sourced from *Navegación Aérea y Aeropuertos Bolivianos (NAABOL)* and the OGIMET platform. Fire hotspot data were derived from satellite records of the *Instituto Nacional de Pesquisas Espaciais (INPE)*, while the Niño 3.4, PDO, and SAM indices were retrieved from specialized international climate repositories. All data were standardized to monthly resolution to ensure temporal comparability between local variables and large-scale climatic forcings.

Validation, Reliability, and Quality Control

The validity of the information was supported by the use of records from technical agencies and platforms with standardized procedures for observation, storage, and dissemination of meteorological and climatic data. Reliability was verified through checks of temporal continuity, internal consistency, detection of missing values, and identification of possible recording anomalies. In cases where gaps or questionable values were identified, conservative correction procedures were applied. For the El Alto station, three outliers corresponding to January 2000 were replaced with the climatological monthly mean of the series. In San José de Chiquitos, missing data were completed through interpolation supported by auxiliary regional stations, prioritizing spatial coherence and temporal continuity. These decisions were adopted to preserve the stability of the series without substantially altering their seasonal structure or low-frequency variability signal.

Data Processing Procedure

Analytical processing was conducted in sequential stages. First, the integrated monthly database was compiled for the four stations and the national fire hotspot series. Second, consistency of formats, units, and temporal coverage was verified for each variable. Third, quality control was performed through inspection of continuity, detection of gaps, and review of anomalous values. Fourth, homogeneous series with monthly resolution were generated, and a unified analytical matrix was structured for the period 2000–2025. Finally, statistical procedures were applied to assess trends, serial dependence, seasonal characterization, and lagged associations with global climate indices.

Statistical Analysis Techniques

The statistical analysis was structured into three complementary components. First, a descriptive characterization of the time series was conducted using measures of central tendency, dispersion, and shape, with the aim of identifying ranges of variation, intra-annual heterogeneity, and the presence of asymmetries. To assess long-term monotonic changes, Sen's slope estimator was applied, given its non-parametric robustness against extreme values and suitability for climatological series.

Second, the temporal structure of the series was examined through autocorrelation functions (ACF) and the Ljung–Box test. This procedure enabled the identification of short-term persistence, dominant seasonal cycles, and serial dependence at different lags, with particular attention to annual and biennial signals relevant to regional hydroclimatic dynamics. Monthly seasonality was characterized using a Seasonal Variation Index (SVI), defined as a relative deviation of each month with respect to the annual mean behavior of the series. This allowed the identification of months with intensification or attenuation of meteorological signals and heat-focus activity. Positive SVI values indicated monthly magnitudes above the annual mean, whereas negative values reflected relative decreases.

Third, the association between large-scale climate indices and local meteorological variables was evaluated using Pearson's correlation coefficient, with monthly lags ranging from 0 to 5 months. This analysis aimed to explore potential delayed responses between ocean–atmospheric forcings and local variability in Tmax, HRmin, and Vmax. The interpretation of coefficients was carried out in terms of direction and magnitude of the linear association, avoiding causal inferences. All statistical processing and database organization were performed within a specialized digital environment for time-series and climatological analysis.

The seasonality of meteorological variables and hot spots was characterized through the Seasonal Variation Index (SVI), constructed from monthly climatologies for the period 2000–2025. For each variable, monthly climatological means $\bar{X}_m$ were first calculated for each month of the year (m=1,…,12), followed by the estimation of the overall annual climatological mean $\bar{X}$. The index was defined as the deviation of the monthly mean with respect to the annual mean level, according to the following expression:

$$(IVE_m = X_m - \bar{X}).$$

In this formulation, IVE_m represents the seasonal anomaly of month (m), $\bar{X}$ denotes the climatological mean of month (m), and $\bar{X}$ corresponds to the annual climatological

mean of the analyzed variable. Under this definition, positive IVE values indicate months with magnitudes above the annual mean, whereas negative values reflect monthly conditions below the mean level of the series.

This procedure enabled the identification of intra-annual phases of intensification and attenuation for each variable, the delimitation of months with maximum seasonal expression, and the comparison of synchronicity among hot spots, maximum temperature, minimum relative humidity, and maximum wind speed. The choice of this approach followed the classical climatological treatment of seasonality through monthly means and anomalies relative to a reference level, widely applied in hydroclimatic time-series analysis (von Storch & Zwiers, 1999; Wilks, 2019). From an interpretative standpoint, the IVE was not assumed to be a dimensionless normalization index, but rather a measure of seasonal deviation expressed in the original units of each variable, thereby preserving the physical magnitude of the annual cycle. This formulation is consistent with the methodological description provided earlier in the manuscript, where the IVE was defined as a seasonal anomaly derived from monthly climatologies.

The relationship between large-scale climate indices and local meteorological variables was evaluated using Pearson's linear correlation coefficient (*r*), in accordance with the structure of the results table reported for the association objective. The analysis was applied between the Niño 3.4 index, the Pacific Decadal Oscillation (PDO), and the Southern Annular Mode (SAM), and the monthly series of maximum temperature, minimum relative humidity, and maximum wind speed from the selected stations.

The association was examined at two temporal levels. First, contemporaneous correlations (*lag*=0) were estimated, corresponding to the temporal coincidence between the climate index and the meteorological variable in the same month. Second, correlations with positive lags of 1 to 5 months were calculated, with the aim of identifying delayed local atmospheric responses to large-scale ocean–atmospheric forcings. Operationally, a lag of (k) months implied correlating the value of the climate index in month (t) with the value of the meteorological variable in month (t+k), under the assumption of a potential delayed response of the regional climate system.

The statistical significance of the coefficients was assessed using the (t)-test associated with Pearson's correlation, adopting a significance level of α=0,05. The magnitude and direction of the associations were interpreted strictly in statistical terms, avoiding direct causal inferences. Accordingly, positive coefficients were interpreted as direct covariation between the index and the meteorological variable, while negative coefficients indicated inverse covariation.

Given that monthly climatological series may exhibit serial dependence, the interpretation of results was carried out jointly with the evidence of autocorrelation previously documented through ACF and the Ljung–Box test, in order to avoid overinterpretation of weak or spurious associations, as recommended by Kendall (1975), Chatfield (2004), Box, Jenkins, Reinsel, & Ljung (2016), and Wilks (2019).

Ethical Considerations

From an ethical standpoint, the research relied exclusively on aggregated, secondary, and publicly accessible environmental data obtained from institutional repositories and

specialized technical platforms. Principles of scientific integrity were observed throughout the process, including documentation of quality control, traceability of processing, verification of homogeneity, and preservation of the original structure of the datasets. In this way, the methodology combined statistical consistency, climatological grounding, and analytical transparency to comparatively examine the relationship between fire hotspots, local meteorological variability, and large-scale climatic teleconnections in Bolivia.

RESULTS

This chapter presents the findings derived from the analysis of seasonal variability in fire hotspots in Bolivia and their relationship with meteorological variables and global climate indices for the period 2000–2025. The discussion begins with the characterization of monthly series of fire hotspots and local variables—maximum temperature, minimum relative humidity, and maximum wind speed—at the stations of El Alto, Cochabamba, Viru Viru, and San José de Chiquitos. This initial analysis enables the identification of trends, seasonality, and periodicities, as well as the magnitude of variability and dispersion, through descriptive statistics and Sen's slope estimator. These results provide the fundamental basis for subsequent calculation of the Seasonal Variation Index (SVI) and the evaluation of associations with large-scale phenomena such as Niño 3.4, PDO, and SAM.

Descriptive Characterization and Monotonic Trends of Monthly Series

Table 2 summarizes descriptive statistics and Sen's slope estimates for monthly meteorological variables and the fire hotspot series. The results reveal marked spatial heterogeneity among stations, consistent with altitudinal and bioclimatic contrasts between the Altiplano, Valleys, and eastern lowlands. For maximum temperature, monthly means were ordered from lowest to highest in El Alto (18.78 °C), Cochabamba (31.07 °C), Viru Viru (34.31 °C), and San José de Chiquitos (36.92 °C), with low coefficients of variation (0.06–0.14), indicating a limited relative variability with respect to the mean. Minimum humidity showed greater relative dispersion, with means ranging from 37.47% in El Alto to 54.18% in Viru Viru, and high amplitudes of intra-annual variation. Maximum wind speed showed the greatest variability in Cochabamba, which recorded both the absolute maximum (103.8 km/h) and minimum (5.2 km/h), as well as the widest range (98.6 km/h) and highest standard deviation (19.19 km/h). Viru Viru, in contrast, concentrated the highest typical values for this variable (mean = 69.69 km/h).

In terms of distributional shape, several series exhibited skewness and kurtosis values deviating from approximate symmetry. Maximum temperature in El Alto was notable for its positive skewness (2.69) and high kurtosis (10.98). Similarly, the fire hotspot series displayed pronounced positive skewness (3.071) and elevated kurtosis (11.465), indicating a concentration of relatively low monthly values interspersed with sporadic extreme episodes of large magnitude. In this latter series, the minimum was 33, the maximum 34,574, the median 686, and the mean 3,117.34, with a standard deviation of 5,380.84 and a coefficient of variation of 0.57—patterns consistent with strong monthly irregularity and the presence of extreme months.

Table 2: Descriptive Statistics and Monotonic Trend (Sen's Slope) of Monthly Meteorological Variables by Station, 2000–2025 (n = 312)

Metereological Station	Variable	Minimum	Maximum	Range	Median	Mean	SD	Variance	CV	Skewness	Kurtosis	Sen's Slope
El Alto	Maximum Temperature (°C)	14,20	33,80	19,60	18,40	18,78	2,69	7,22	0,14	2,69	10,98	0,00
El Alto	Minimum Relative Humidity (%)	10,80	75,70	64,90	34,20	37,47	16,86	284,10	0,45	0,36	-1,02	-0,05
El Alto	Maximum Wind Speed (km/h)	12,40	77,80	65,40	50,00	48,63	10,76	115,74	0,22	-0,98	2,28	0,00
Cochabamba	Maximum Temperature (°C)	27,20	40,50	13,30	30,80	31,07	1,81	3,26	0,06	0,83	2,07	0,00
Cochabamba	Minimum Relative Humidity (%)	15,00	58,50	43,50	39,15	38,70	8,85	78,39	0,23	-0,10	-0,45	-0,05
Cochabamba	Maximum Wind Speed (km/h)	5,20	103,80	98,60	37,10	31,87	19,19	368,31	0,60	0,29	-0,91	0,08
Viru Viru	Maximum Temperature (°C)	29,40	41,50	12,10	34,40	34,31	2,23	4,96	0,06	0,16	-0,16	0,00
Viru Viru	Minimum Relative Humidity (%)	22,00	88,20	66,20	56,80	54,18	13,98	195,46	0,26	-0,24	-0,86	-0,03
Viru Viru	Maximum Wind Speed (km/h)	40,40	101,90	61,50	70,40	69,69	9,66	93,35	0,14	0,09	0,10	0,00
San José de Chiquitos	Maximum Temperature (°C)	28,00	44,10	16,10	37,00	36,92	2,75	7,55	0,07	-0,30	0,30	0,01
San José de Chiquitos	Minimum Relative Humidity (%)	21,60	71,80	50,20	45,75	45,61	10,47	109,43	0,23	0,04	-0,50	0,02
San José de Chiquitos	Maximum Wind Speed (km/h)	8,00	74,10	66,10	23,55	29,39	15,21	231,25	0,52	0,71	-0,78	-0,02
Fire hotspots		33,00	34574,00	34541,00	686,00	3117,34	5380,84	28953468,32	0,57	3,07	11,47	0,78

Note: SD = standard deviation; CV = coefficient of variation (SD/Mean). A decimal comma and uniform rounding to two decimals were applied. Sen's slope is a non-parametric estimator of monotonic trend; its units correspond to the variable per unit of time in the series (e.g., °C/month, %/month, km/h/month).

Monotonic trends estimated using Sen's slope were generally of low magnitude. Most meteorological series yielded values close to zero, although slight decreases were observed in minimum relative humidity at El Alto (−0.05), Cochabamba (−0.05), and Viru Viru (−0.03). Small increases were detected in maximum temperature at San José de Chiquitos (0.01) and in maximum wind speed at Cochabamba (0.08). For the fire hotspot series, Sen's slope was positive (0.78), describing a net increase in monthly counts during the study period. Consequently, the dominant feature of the dataset was not a strong linear trend but rather the coexistence of regional contrasts, distributional asymmetry, and extreme high-magnitude episodes, particularly in fire hotspots.

Intra-Annual Monthly Distribution of Meteorological Variables

Figure 2 presents the monthly distribution of maximum temperature, minimum relative humidity, and maximum wind speed at the study stations, with the purpose of visually characterizing the seasonal progression of local meteorological variables and complementing the quantitative evidence provided in subsequent tables.

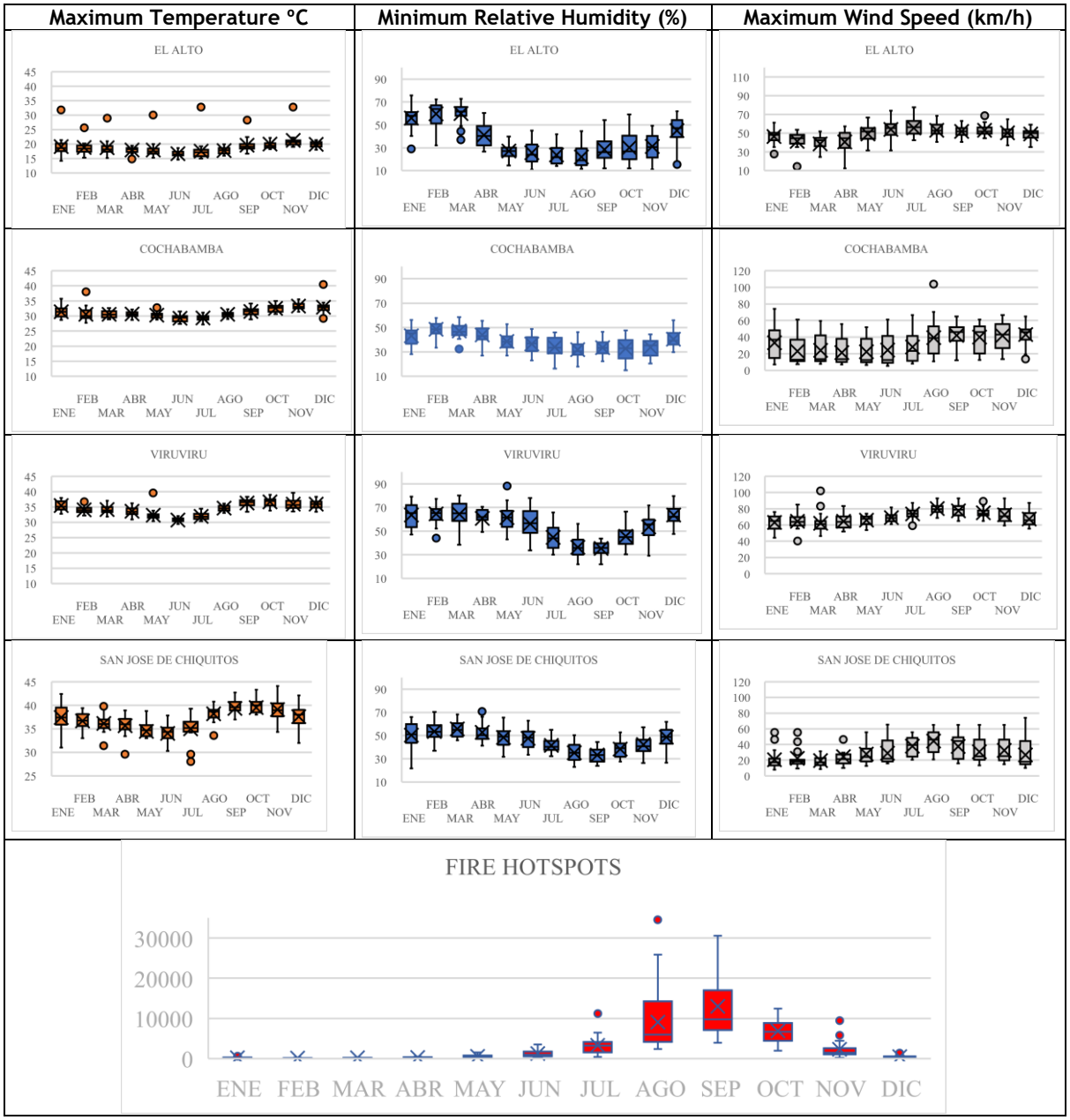

Figure 2: Monthly distribution of maximum temperature (°C), minimum relative humidity (%), and maximum wind speed (km/h) at the study stations (2000–2025).

Serial Dependence and Seasonal Periodicity

Figure 3 and Table 3 show that the monthly series exhibit statistically detectable temporal dependence and a periodic organization dominated by the annual signal. Table 3 summarizes autocorrelation at key lags (1, 12, and 24 months) together with the cumulative Ljung–Box statistics; therefore, this section should be interpreted as evidence of serial persistence and seasonality, rather than as a Mann–Kendall type trend test.

Across all variables and stations, the values of Q(12) and Q(24) were high, with $p<.001$, confirming that the temporal structure departed from randomness at both annual and biennial scales.

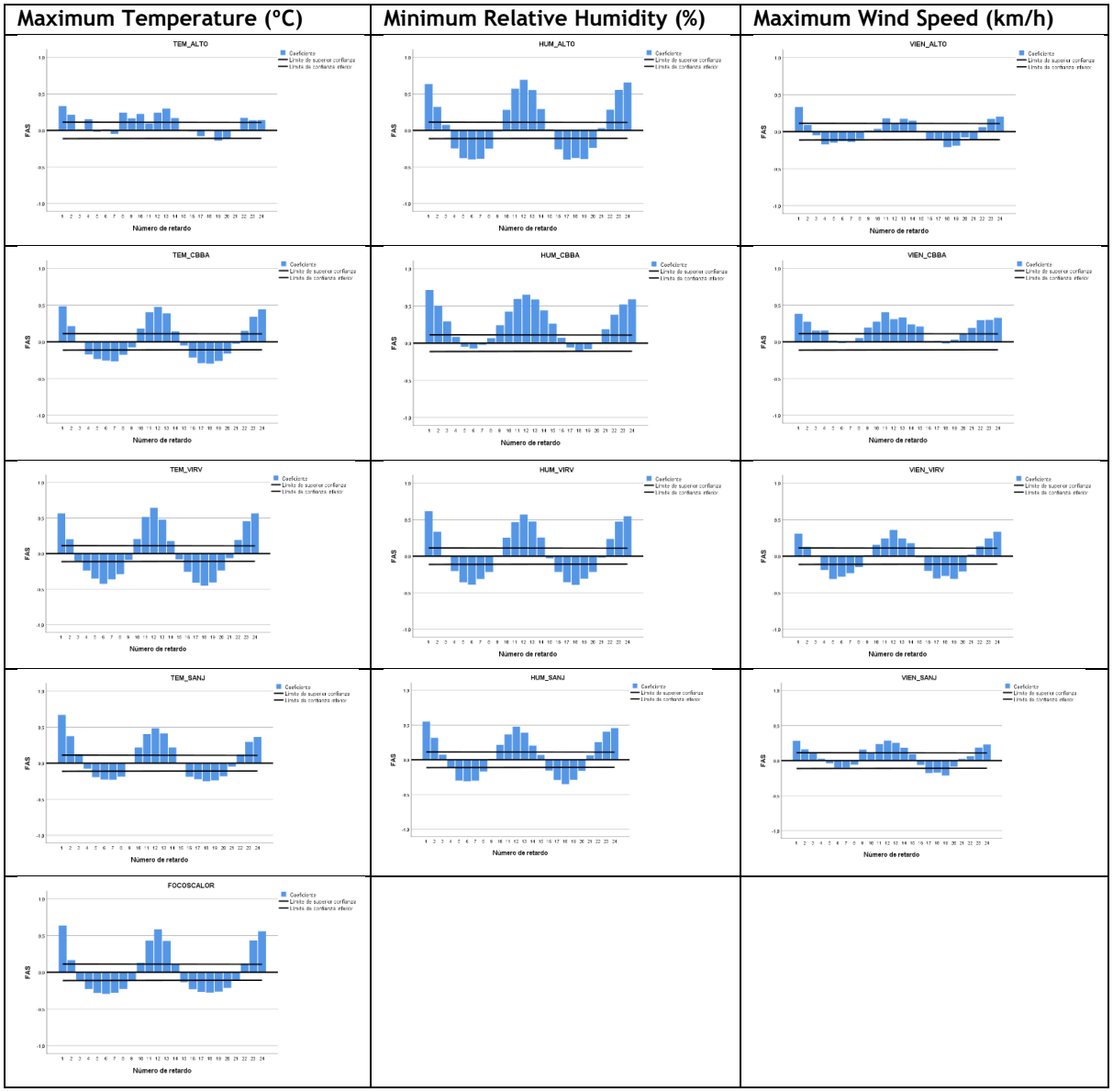

Figure 3: Dominant Periodicity of Monthly Series by Meteorological Variable, 2000-2025

Note: The "dominant periodicity" is reported in months (e.g., 12 = annual; 6 = semiannual; 24 = biennial), estimated from the structure of temporal dependence (e.g., peaks in ACF/PACF and/or complementary diagnostics).

For maximum temperature, short-term persistence was moderate to high, with r1values between 0.33 and 0.67, and the annual signal was clear, with r12 values between 0.24 and 0.64. The strongest annual seasonality was observed at Viru Viru (r12 = 0,64) and Cochabamba (r12 = 0,48), whereas El Alto exhibited a more moderate annual structure (r12 = 0,24).

Minimum relative humidity displayed the most regular organization of the dataset, with r1 values between 0.55 and 0.71 and r12 values between 0.48 and 0.69. El Alto stood out with the highest annual autocorrelation (r12 = 0,69) and biennial autocorrelation (r24 =

0,65). In contrast, maximum wind speed showed weaker and more heterogeneous seasonality, with r12 values between 0.12 and 0.36 and r1 values between 0.28 and 0.38.

The fire hotspot series also exhibited a defined periodic structure, with r1 = 0,64, r12 = 0,59 y r24 = 0,56, along with high and significant Ljung–Box values at 12 and 24 months. This pattern indicates strong annual recurrence reinforced by a secondary biennial signal. Operationally, the dominant periodicity of the phenomenon was annual, with additional support at the 24-month lag for several variables and stations.

Table 3: Autocorrelation at Seasonal Lags and Ljung-Box Test in Monthly Series (2000-2025)

Metereological Station	Variable	r_1 (ACF)	r_{12} (ACF)	Q(12)	p(12)	r_{24} (ACF)	Q(24)	p(24)
El Alto	MaximumTemperature (°C)	0,33	0,24	124,69	< .001	0,12	199,77	< .001
El Alto	Minimum Relative Humidity (%)	0,64	0,69	633,47	< .001	0,65	1231,61	< .001
El Alto	Maximum Wind Speed (km/h)	0,33	0,12	84,38	< .001	0,20	166,89	< .001
Cochabamba	MaximumTemperature (°C)	0,49	0,48	308,69	< .001	0,44	583,47	< .001
Cochabamba	Minimum Relative Humidity (%)	0,71	0,65	604,09	< .001	0,59	1084,26	< .001
Cochabamba	Maximum Wind Speed (km/h)	0,38	0,31	207,93	< .001	0,33	389,95	< .001
Viru Viru	MaximumTemperature (°C)	0,57	0,64	538,98	< .001	0,57	1037,62	< .001
Viru Viru	Minimum Relative Humidity (%)	0,62	0,57	500,69	< .001	0,55	950,16	< .001
Viru Viru	Maximum Wind Speed (km/h)	0,31	0,36	197,26	< .001	0,34	407,83	< .001
San José de Chiquitos	MaximumTemperature (°C)	0,67	0,49	395,16	< .001	0,36	626,19	< .001
San José de Chiquitos	Minimum Relative Humidity (%)	0,55	0,48	362,56	< .001	0,46	689,88	< .001
San José de Chiquitos	Maximum Wind Speed (km/h)	0,28	0,29	102,39	< .001	0,23	207,88	< .001
Fire hotspots		0,64	0,59	433,96	< .001	0,56	788,21	< .001

Note: ACF = autocorrelation function; r1, r12 y r24 = autocorrelation at lags of 1, 12, and 24 months; (Q(m)) = Ljung–Box statistic accumulated up to lag (m); (p) = asymptotic significance (x^2).

Intra-Annual Seasonal Structure via the Seasonal Variation Index (SVI)

Table 4 summarizes the relative monthly magnitudes of the variables through the SVI. Since the SVI was defined as the deviation of each monthly mean from the annual mean, positive values indicate months above the average level of the series, while negative values correspond to months below the annual mean.

For maximum temperature, the seasonal pattern was consistent across regions, with relative maxima concentrated in September–October. It can be stated with confidence that the relative thermal increase culminates toward the end of the dry season in all regions analyzed. For minimum relative humidity, the most intense negative anomalies were concentrated between July and September, with critical values observed at Viru Viru (SVI = −18.99) and El Alto (SVI = −15.37). This reflects a marked intra-annual hygrometric deficit during this portion of the year.

The fire hotspot series exhibited highly concentrated seasonality. Between January and June, SVI values were persistently negative, with minimum anomalies between February and May. In July, the index approached zero, followed by a rapid transition to strongly positive values in August (5,885.42) and September (9,875.70), then a decline in October (3,828.80), and a return to negative values in November and December. This behavior describes a unimodal critical window, with a principal peak in September and activation already visible in August. Therefore, monthly fire activity was concentrated in the August–October quarter, coinciding with the period of elevated maximum temperatures and reduced minimum relative humidity.

Table 4: Seasonal Variation Index (SVI) by month and meteorological station (2000–2025).

Variable / Station	JAN	FEB	MAR	APR	MAY	JUN	JUL	AUG	SEP	OCT	NOV	DEC
Maximum Temperature (°C)												
El Alto	-0,17	-0,26	0,02	-0,79	-0,69	-1,96	-1,23	-0,96	0,83	1,28	2,83	1,12
Cochabamba	0,41	-0,79	-0,46	0,43	-0,81	-1,74	-1,77	-0,54	0,46	1,51	2,27	1,89
Viru Viru	1,08	-0,25	-0,13	-0,80	-1,91	-3,58	-2,36	0,29	2,02	2,32	1,62	1,68
San José	0,53	-0,17	-0,66	-1,24	-2,43	-2,79	-1,81	1,38	1,47	2,66	2,24	0,82
Minimum Relative Humidity (%)												
El Alto	18,46	22,13	22,43	3,53	-10,34	-11,67	-13,67	-15,37	-9,16	-7,23	6,33	7.43
Cochabamba	4,39	9,82	8,69	5,34	-0,25	-2,12	-4,71	-6,75	-5,20	-6,03	-5,04	1,85
Viru Viru	10,10	10,50	10,50	6,47	7,70	1,69	-9,33	-17,91	-18,99	-8,74	-0,81	8,83
San José	4,92	7,84	9,88	7,48	3,09	1,88	-4,07	-10,57	-12,38	-7,24	-3,55	2,71
Maximum Wind Speed (km/h)												
El Alto	-2,60	-7,01	-10,17	-7,19	0,71	4,84	6,96	4,31	3,20	4,40	1,72	0,81
Cochabamba	1,14	-8,96	-7,28	-10,62	-9,34	-7,23	-3,80	7,27	9,91	7,67	9,58	11,66
Viru Viru	-5,93	-5,25	-7,78	-4,81	-3,78	-0,98	4,04	10,61	7,94	5,41	2,76	-2,22
San José	-8,84	-7,13	-10,22	-4,46	-1,66	-1,49	8,31	15,11	8,26	1,24	3,30	-2,41
Fire hotpots (IVE)												
Total (unspecified)	-2894,85	-3003,51	-2965,07	-2869,43	-2532,81	-1976,63	66,84	5885,42	9875,70	3828,80	-759,60	-2654,86

Note: Positive values indicate magnitudes above the annual mean of the series, while negative values denote relative decreases.

Taken together, the seasonal information indicates that the phase of greatest atmospheric susceptibility to fire occurrence is located at the end of the dry season, when the system combines positive thermal anomalies, hygrometric deficit, and, in several regions, relative increases in wind speed. The SVI evidence thus supports a clear temporal delineation of the period of greatest fire activity, with visible hotspot maxima in September and a preceding rise in August, rather than two equivalent peaks.

Association Between Global Climate Indices and Local Meteorological Variables

Table 5 presents Pearson correlation coefficients between the Niño 3.4, PDO, and SAM indices and local meteorological variables at lags of 0 to 5 months. Since the table does not report individual *p*-values for each coefficient, the results must be interpreted in terms of direction and magnitude of linear association, rather than as evidence of specific statistical significance for each cell.

Furthermore, this matrix corresponds exclusively to maximum temperature, minimum relative humidity, and maximum wind speed. Consequently, it is not methodologically correct to attribute in this section a direct correlation between Niño 3.4 and fire hotspots, as such a relationship is not included in the table presented.

Regarding maximum temperature, the clearest pattern was associated with the Niño 3.4 index. The Cochabamba station exhibited the strongest positive associations, with a progressive increase from lag 0 ($r = 0.210$) to peaks at lags 2 and 3 months ($r = 0.283$), maintaining similar values up to lag 5. This pattern suggests a more pronounced delayed thermal response in the Valleys compared to other regions. In Viru Viru and San José de Chiquitos, positive correlations were weaker but increased with lag, reaching 0.154 and 0.132, respectively, whereas in El Alto coefficients remained close to zero. With respect to PDO, maximum temperature showed predominantly negative associations in Viru Viru and San José de Chiquitos, being more intense in the latter, where the minimum was observed at lag 4 ($r = -0.170$). In relation to SAM, thermal correlations were generally weak and mostly negative, without a spatially defined pattern comparable to that observed for Niño 3.4.

Table 5: Pearson correlation coefficients (r) between climate indices and meteorological variables by monthly lags.

	INDICES	CORRELATION r	El Alto	Cochabamba	Viru Viru	San José de Chiquitos
Maximum Temperature (°C)	Niño 3.4	0 - 0	.008	.210	.040	.098
		0 - 1	.036	.251	.067	.108
		0 - 2	.034	.283	.101	.132
		0 - 3	.073	.283	.128	.128
		0 - 4	.085	.280	.130	.118
		0 - 5	.087	.280	.154	.085
	PDO	0 - 0	-.080	.032	-.070	-.150
		0 - 1	-.070	.042	-.040	-.140
		0 - 2	-.040	.027	-.070	-.150
		0 - 3	-.050	.000	-.090	-.160
		0 - 4	-.050	-.020	-.090	-.170
		0 - 5	-.010	-.020	-.080	-.160
	SAM	0 - 0	-.070	-.010	.000	-.040
		0 - 1	-.020	-.070	-.030	.005
		0 - 2	-.040	-.050	-.140	-.040
		0 - 3	-.070	-.110	-.080	-.050
		0 - 4	-.060	-.040	-.050	.003
		0 - 5	-.010	.008	-.010	.022
Minimum Relative Humidity (%)	Niño 3.4	0 - 0	-.017	-.135	.058	.070
		0 - 1	-.019	-.169	.013	.029
		0 - 2	-.042	-.180	-.020	.001
		0 - 3	-.052	-.171	-.034	-.012
		0 - 4	-.042	-.151	-.034	-.011
		0 - 5	-.064	-.144	-.026	.006
	PDO	0 - 0	-.029	.031	.103	.015
		0 - 1	-.013	.012	.107	.005
		0 - 2	-.006	.000	.108	.020
		0 - 3	-.021	-.026	.055	-.022
		0 - 4	-.027	-.043	.041	-.019
		0 - 5	-.024	-.045	.010	-.062
	SAM	0 - 0	-.169	.033	.019	.100
		0 - 1	-.230	-.020	.021	.141
		0 - 2	-.190	-.035	.037	.080
		0 - 3	-.133	-.126	-.051	.011
		0 - 4	-.167	-.191	-.123	-.041
		0 - 5	-.076	-.203	-.128	-.084
Maximum Wind Speed (km/h)	Niño 3.4	0 - 0	-.009	.077	.108	.053
		0 - 1	.027	.096	.120	.070
		0 - 2	.039	.112	.103	.050
		0 - 3	.035	.094	.084	.044
		0 - 4	.015	.108	.060	.034
		0 - 5	.000	.087	.008	.011
	PDO	0 - 0	-.012	-.033	.004	.109
		0 - 1	.015	-.063	.030	.139
		0 - 2	.017	-.085	.022	.151
		0 - 3	-.040	-.072	-.027	.105
		0 - 4	-.025	-.071	-.009	.072
		0 - 5	.021	-.054	-.007	.074
	SAM	0 - 0	-.021	.002	-.175	-.108
		0 - 1	-.055	-.007	-.114	-.085
		0 - 2	-.092	.027	-.103	-.156
		0 - 3	-.029	.015	-.092	-.103
		0 - 4	.012	.014	-.036	-.052
		0 - 5	.163	.057	.124	.009

Note: The values represent the Pearson correlation coefficient (r). Own elaboration based on meteorological data.

For minimum humidity, Niño 3.4 exhibited stronger negative associations in Cochabamba, with a minimum at lag 2 (r = −0.180), while in El Alto coefficients were weak and in lowland stations tended to approach zero. PDO correlations were small, with a moderate positive signal only in Viru Viru during early lags (up to r = 0.108), and values close to zero or slightly negative in the other stations. The most consistent pattern for this variable was observed with SAM in El Alto, where correlations were negative across all lags and reached their maximum magnitude at lag 1 (r = −0.230). In Cochabamba, an inverse association with SAM also predominated, becoming more evident at lags 4 and 5 (r = −0.191 and −0.203). In San José de Chiquitos, the signal was initially positive but weakened until becoming negative at later lags. Consequently, minimum humidity displayed a spatially

differentiated response, with greater sensitivity to SAM in the Altiplano and to Niño 3.4 in the Valleys.

For maximum wind speed, associations were generally weaker than those observed for maximum temperature and minimum humidity. Niño 3.4 showed modest positive correlations in Cochabamba and Viru Viru, with maxima of 0.112 and 0.120, respectively, while in El Alto values remained close to zero. PDO presented a contrasting signal: weak negative associations in El Alto, Cochabamba, and Viru Viru, and positive associations in San José de Chiquitos, where it reached 0.151 at lag 2. Regarding SAM, the behavior was more heterogeneous; negative coefficients were recorded in Viru Viru and San José de Chiquitos during early lags, while in El Alto a relatively higher positive value appeared at lag 5 ($r = 0.163$). Overall, maximum wind speed exhibited a weaker and less stable connection with large-scale climate indices compared to the other local variables.

In summary, the correlation matrix indicates that local responses to global climate indices were heterogeneous across variables and regions. Niño 3.4 was primarily associated with maximum temperature in Cochabamba and, to a lesser extent, with the reduction of minimum humidity in the same station. SAM presented the clearest inverse signal with minimum humidity in El Alto, while PDO showed more evident negative thermal associations in San José de Chiquitos. Nevertheless, given that the table does not provide significance tests for each coefficient, these associations should be interpreted as patterns of linear covariation rather than conclusive evidence of statistically confirmed teleconnections at individual lags.

DISCUSSION

The analysis of results supports the argument that meteorological dynamics associated with fire activity in Bolivia are primarily governed by a robust internal seasonal structure rather than by a single dominant climatic forcing. The persistence of significant autocorrelations at lags of 12 and 24 months, together with the concentration of the Seasonal Variation Index of fire hotspots between August and October, indicates that the system exhibits a recurrent temporal organization rather than random behavior. Climatologically, this reveals that monthly fire activity is embedded within a recurrent dry window characterized by the convergence of maximum temperatures, minimum hygrometric values, and, in several stations, a relative increase in ventilation. This interpretation is consistent with the regional climatology described for Bolivia by Seiler et al. (2013), who documented marked hydroclimatic seasonality and strong spatial contrasts, as well as with continental syntheses that highlight the increased fire hazard in South America during the dry season, when dry atmospheric conditions, hydric stress, and the availability of fine dry fuels coincide (Burton et al., 2021).

From a meteorological perspective, the synchrony between the rise in maximum temperature toward September–October and the decline in minimum humidity between July and September suggests that the critical annual phase results from the superposition of two complementary processes: progressive warming of near-surface air and seasonal desiccation of the environment. This configuration aligns with South American fire literature, which emphasizes that the occurrence and severity of wildfires depend on the combination of warm, dry, and, in certain contexts, windy conditions, rather than on the isolated action of a single atmospheric variable (Burton et al., 2021). In Bolivia, Maillard et al. (2020) and

Singh et al. (2022) have shown that meteorological drought and the dry seasonality of eastern Bolivia favor fire occurrence, particularly when interacting with landscape fragmentation and anthropogenic disturbance. Accordingly, the results reinforce the interpretation that fire seasonality in Bolivia should be understood as a seasonal atmospheric convergence, upon which fuel, land use, and ignition factors subsequently act.

In the field of teleconnections, the most consistent signal corresponded to Niño 3.4 in relation to maximum temperature, especially in Cochabamba, where positive correlations reached their greatest magnitude at lags of 2 to 5 months. Although coefficients were moderate, the pattern is physically plausible, as it suggests a delayed thermal response to equatorial Pacific anomalies. This interpretation concurs with evidence that ENSO constitutes one of the principal modulators of hydroclimatic variability in South America and Bolivia, with differentiated effects depending on region, season, and variable analyzed (Seiler et al., 2013). It also coincides with Amazonian and continental studies linking drought episodes and increased fire activity to large-scale oceanic anomalies, particularly when ENSO favors relatively warmer and drier conditions in tropical and subtropical sectors (Aragão et al., 2007; Burton et al., 2021). In this sense, the observed signal should not be interpreted as deterministic control, but rather as regional thermal modulation compatible with mechanisms already described for the continent.

The SAM signal on minimum humidity, particularly the inverse coupling detected in El Alto and, to a lesser extent, in Cochabamba, warrants a cautious but conceptually relevant interpretation. Dynamically, this pattern suggests that part of the hygrometric variability in western Bolivia may be linked to reorganizations of Southern Hemisphere circulation. Hendon et al. (2014) demonstrated that SAM modifies subtropical precipitation distribution through latitudinal shifts in westerly winds and cyclonic activity, thereby affecting moisture availability across hemispheric bands. Although this framework was not formulated specifically for Bolivia, it provides a reasonable dynamic basis for interpreting the possible relationship between a SAM phase and drier conditions in Andean or subtropical sectors. Complementarily, Gomes et al. (2021) documented that the negative phase of SAM during the 2019/2020 drought was associated with subtropical subsidence and precipitation alterations over South America. Consequently, this finding should be considered as an indication of extratropical modulation of the regional hygrometric balance, rather than as conclusive causal evidence.

By contrast, PDO exhibited weaker and less spatially uniform associations, although relatively more visible negative thermal correlations were observed in San José de Chiquitos. This behavior suggests that, during the analyzed period, PDO acted mainly as a low-frequency background modulator rather than as a dominant driver of local monthly variability. Such an interpretation is consistent with regional literature, which generally attributes to PDO a modulatory influence on the interannual Pacific signal, without expecting direct and homogeneous responses in local monthly meteorological variables (Burton et al., 2021). Its role should therefore be maintained as a complementary component within the teleconnection framework, without overemphasis.

Another relevant finding is that the fire hotspot series exhibited strong positive skewness, high kurtosis, and highly concentrated seasonality, with a peak in September. This pattern indicates that fire activity depends not only on the annual cycle but also on the episodic occurrence of extraordinarily intense months. Regional literature supports this

interpretation: Aragão et al. (2007) showed that dry years in the Amazon generate nonlinear fire responses, while Maillard et al. (2020) and Singh et al. (2022) emphasize that severe droughts and anthropogenic disturbance in Bolivia amplify wildfire severity and extent. Therefore, the identified annual signal should not be understood as a closed mechanical regularity, but rather as a recurrent climatic basis upon which extreme episodes and territorial factors intensify the fire system's response.

From an applied perspective, the results suggest that joint monitoring of maximum temperature, minimum humidity, and selected large-scale indices—particularly Niño 3.4 and SAM—could improve the identification of periods of heightened meteorological susceptibility. However, given that observed correlations were of low to moderate magnitude, this utility should be understood as potential rather than as demonstrated predictive capacity. Methodologically, operational application would require further validation through explicit predictive models, out-of-sample evaluation, and incorporation of precipitation, fuel, and anthropogenic ignition variables, in line with recommendations by Burton et al. (2021) and Devisscher et al. (2016). In summary, the evidence supports three central conclusions: fire activity in Bolivia is strongly structured by the seasonal cycle; the August–October period concentrates the greatest meteorological hazard; and local variability exhibits differentiated associations with Niño 3.4, SAM, and, to a lesser extent, PDO.

CONCLUSIONS

The joint analysis of monthly fire hotspot series and local meteorological variables in Bolivia revealed that the temporal dynamics of the phenomenon were dominated by a marked seasonal structure, with a persistent annual signal and, in several cases, a secondary biennial periodicity. In this regard, the study demonstrated that the series of maximum temperature, minimum humidity, maximum wind speed, and fire hotspots did not exhibit random behavior, but rather a recurrent temporal organization over the 2000–2025 period, with consistent regional differences among the Altiplano, Valleys, and eastern lowlands. Thus, the trend, seasonality, and periodicity of monthly series were characterized for the stations of El Alto, Cochabamba, Viru Viru, and San José de Chiquitos.

With respect to intra-annual seasonality, the calculation of the Seasonal Variation Index (SVI) allowed for clear identification of the months with the greatest relative magnitude of meteorological variables and fire hotspots. In general terms, maximum temperature reached its strongest positive anomalies toward the end of the dry season, mainly between September and October, while minimum humidity exhibited its most intense negative anomalies between July and September. The fire hotspot series showed a sharply defined seasonal concentration, with activation beginning in August, a principal peak in September, and subsequent decline in October. Consequently, the SVI enabled the delineation of a critical seasonal window of heightened meteorological hazard, associated with the concurrence of atmospheric warming, reduction in relative humidity, and increased fire activity.

Regarding the relationship between large-scale climatic variability and regional meteorological dynamics, the results indicated that associations were heterogeneous across variables and regions. The Niño 3.4 index exhibited the strongest positive correlations with maximum temperature, particularly in Cochabamba, with a more evident response at lags

of 2 to 5 months. SAM displayed the clearest inverse signal with minimum humidity, especially in El Alto, while PDO showed weaker and less spatially uniform associations. Taken together, these findings suggest that part of local meteorological variability is differentially associated with large-scale ocean–atmosphere forcings, although with predominantly low to moderate magnitudes.

It is therefore concluded that the monthly dynamics of fire hotspots in Bolivia between 2000 and 2025 were strongly conditioned by regional climatic seasonality, particularly by the convergence of thermal maxima and hygrometric minima during the final stage of the dry season. Furthermore, the evidence suggests that large-scale variability, expressed through Niño 3.4, PDO, and SAM, is differentially related to local meteorological variability, providing a useful interpretive framework for understanding the atmospheric configuration preceding periods of heightened fire activity. Accordingly, the study contributes a relevant climatological basis for strengthening seasonal monitoring schemes and early warning systems aimed at wildfire risk management in Bolivia.

Finally, from a methodological perspective, it is concluded that the integration of monthly time series, autocorrelation, the Ljung–Box test, and the Seasonal Variation Index constitutes a useful approach for characterizing intra-annual dynamics and the temporal organization of meteorological variables and fire hotspots. Nevertheless, to strengthen the study's inferential capacity, future research should explicitly incorporate the analysis of associations between fire hotspot SVIs and global climate indices, as well as include complementary variables such as precipitation, fuel availability, and anthropogenic pressure, in order to construct a more comprehensive explanation of the fire regime across Bolivia's diverse biomes.

REFERENCES

Aragão, L. E. O. C., Malhi, Y., Roman-Cuesta, R. M., Saatchi, S., Anderson, L. O., & Shimabukuro, Y. E. (2007). Spatial patterns and fire response of recent Amazonian droughts. Geophysical Research Letters, 34(7), L07701. https://doi.org/10.1029/2006GL028946

Arguez, A., Bissolli, P., Ganter, C., Martinez, R., Mekonnen, A., Stevens, L., & Zhu, Z. (Eds.). (2025). State of the Climate in 2024: Regional climates [Special supplement]. Bulletin of the American Meteorological Society, 106(8). https://doi.org/10.1175/2025BAMSStateoftheClimate_Chapter7.1

Box, G. E. P., Jenkins, G. M., Reinsel, G. C., & Ljung, G. M. (2016). Time series analysis: Forecasting and control (5th ed.). Wiley.

Burton, C., Kelley, D. I., Jones, C. D., Betts, R. A., Cardoso, M., & Anderson, L. (2021). South American fires and their impacts on ecosystems increase with continued emissions. Climate Resilience and Sustainability, 1, e8. https://doi.org/10.1002/cli2.8

Cardil, A., Rodrigues, M., Tapia, M., Barbero, R., Ramírez, J., Stoof, C. R., Silva, C. A., Mohan, M., & de-Miguel, S. (2023). Climate teleconnections modulate global burned area. Nature Communications, 14(1), Article 427. https://doi.org/10.1038/s41467-023-36052-8

Chatfield, C. (2004). The analysis of time series: An introduction (6th ed.). Chapman & Hall/CRC. https://doi.org/10.4324/9780203491683

Devisscher, T., Anderson, L. O., Aragão, L. E. O. C., Galván, L., & Malhi, Y. (2016). Increased wildfire risk driven by climate and development interactions in the Bolivian Chiquitania, southern Amazonia. PLOS ONE, 11(9), e0161323. https://doi.org/10.1371/journal.pone.0161323

Gomes, M. S., Cavalcanti, I. F. de A., & Müller, G. V. (2021). 2019/2020 drought impacts on South America and atmospheric and oceanic influences. Weather and Climate Extremes, 34, 100404. https://doi.org/10.1016/j.wace.2021.100404

Hendon, H. H., Lim, E.-P., & Nguyen, H. (2014). Seasonal variations of subtropical precipitation associated with the Southern Annular Mode. Journal of Climate, 27(9), 3446–3460. https://doi.org/10.1175/JCLI-D-13-00550.1

Ibisch, P. L., & Mérida, G. (Eds.). (2003). Biodiversidad: La riqueza de Bolivia. Estado de conocimiento y conservación. Editorial FAN.

Kendall, M. G. (1975). Rank correlation methods (4th ed.). Charles Griffin. https://archive.org/details/rankcorrelationm0000kend

Maillard, O., Vides-Almonacid, R., Flores-Valencia, M., Coronado, R., Vogt, P., Vicente-Serrano, S. M., Azurduy, H., Añivarro, R., & Cuéllar, R. L. (2020). Relationship of forest cover fragmentation and drought with the occurrence of forest fires in the Department of Santa Cruz, Bolivia. Forests, 11(9), 910. https://doi.org/10.3390/f11090910

Seiler, C., Hutjes, R. W. A., & Kabat, P. (2013). Climate variability and trends in Bolivia. Journal of Applied Meteorology and Climatology, 52(1), 130–146. https://doi.org/10.1175/JAMC-D-12-0105.1

Singh, M., Sood, S., & Collins, C. M. (2022). Fire dynamics of the Bolivian Amazon. Land, 11(9), 1436. https://doi.org/10.3390/land11091436

von Storch, H., & Zwiers, F. W. (1999). Statistical analysis in climate research. Cambridge University Press. http://hvonstorch.de/klima/books/block/sz.pdf

Wilks, D. S. (2019). Statistical methods in the atmospheric sciences (3rd ed.). Academic Press.